Biophysical Chemistry, 30 (1988) 113–132
Elsevier

BPC 01251

Energization-induced redistribution of charge carriers near membranes *

Frits Kamp **, Yi-der Chen and Hans V. Westerhoff

Laboratory of Molecular Biology, National Institute of Diabetes, and Digestive and Kidney Diseases, National Institutes of Health, Building 2, Room 319, Bethesda, MD 20892, U.S.A.

Received 6 October 1987
Revised manuscript received 9 December 1987
Accepted 11 January 1988

Proton; Chemiosmotic coupling; Poisson-Boltzmann equation; Electric potential; Surface charge; Oxygen pulse; Charge compensation

The electric field arising from proton pumping across a topologically closed biological membrane causes accumulation close to the membrane of ionic charges equivalent to the charge of the pumped protons, positive on the side towards which protons are pumped, negative on the other side. We shall call this the 'active surface charge'. We here use the Poisson-Boltzmann equation to evaluate the effects of zwitterionic buffer molecules and uncharged proteins in the aqueous phase bordering the membrane on the magnitude and ionic composition of the active surface charge. For the positive side of the membrane, the main results are: (1) If the membrane is freely accessible to bulk phase ions, pumped protons exchange with these ions, such that the active surface charge consists of salt cations. (2) If a significant fraction of the ions in bulk solution consists of buffer molecules, then some of the pumped protons will remain close to the membrane and constitute a major fraction of the active surface charge. (3) If a protein layer borders the membrane, a significant part of the transmembrane electric potential difference exists within that protein layer and protons inside this layer dominate the active surface charge. (4) On the negative side of the membrane the corresponding phenomena would occur. (5) All these effects are strictly dependent on the transmembrane electric potential difference arising from proton pumping and would come in addition to the well known effects of buffers and electrically charged proteins on the retention of scalar protons. (6) No additional proton diffusion barrier may be required to account for a deficit in number of protons observed in the aqueous bulk phase upon aeration-induced proton pumping.

* Part of this work has been presented at the 6th European Bioenergetics Conference (1986) in Prague.

Correspondence address: H.V. Westerhoff, Antoni van Leeuwenhoekhuis, Plesmanlaan 121, 1066 CX Amsterdam, The Netherlands.
** Present address: B.C.P. Jansen Institute, Plantage Muidergracht 12, 1018 TV Amsterdam, The Netherlands.

Glossary

Symbols	Meaning	Units
Latin		
A	concentration of acid buffering groups	M
B	concentration of alkaline buffering groups	M
c	concentration	mol m^{-3}
C	electric capacitance	$\mu F\ cm^{-2}$
$Cl^-(x)$	chloride ion concentration at location x	M
l	intramembrane spacing	nm
d_m	membrane thickness	nm
E	electric field strength	V m^{-1}
F	Faraday's constant	C mol^{-1}
G	Gibbs free energy	kJ mol^{-1}
$H^+(x)$	proton concentration at location x	mol m^{-3}

Glossary (continued)

Symbols	Meaning	Units
J	enzyme cycle rate	s^{-1}
k	Boltzmann's constant	$J K^{-1}$
K_a	equilibrium constant of acid buffering groups	M
K_b	equilibrium constant of alkali-buffering groups	M
$K^+(x)$	potassium ion concentration at location x	M
$OH^-(x)$	hydroxyl ion concentration at location x	M
q_e	elementary charge	C
r	radius	nm
r_m	membrane-protein, cf. membrane-water, interphase	nm
r_p	protein-water interphase	nm
R	gas constant	$J K^{-1} mol^{-1}$
T	temperature	K
x	x coordinate in space	m
z_i	number of elementary charges carried by ion i	
Greek		
α, β	constant	
δ	dielectric increment	–
$\epsilon = \epsilon_0 \epsilon_r$	dielectric constant	$N^{-1} m^{-2} C^2$
ϵ_r	relative dielectric constant	–
ϵ_0	dielectric constant of vacuum	$N^{-1} m^{-2} C^2$
ψ	reduced potential	–
λ	constant	
κ	1/Debye-Hückel length	m^{-1}
π	partition coefficient	–
ρ	charge density	$C m^{-3}$
σ	excess surface charge density	$C m^{-2}$
$\tilde{\mu}$	electrochemical potential	$J mol^{-1}$
ψ	electric potential	V
$\Delta\psi = \Delta\psi_b$	bulk-to-bulk electric potential difference	V
$\Delta\psi_m$	transmembrane electric potential difference	V
Subscripts		
b	bulk	
Cl	chloride	
e	electron	
eq	equilibrium	
H	proton	
i	ionic species i	
K	potassium	
m	membrane	
0	vacuum	
p	protein	
pol	polarization	
r	relative	
w	water	
Operators		
∇	$\vec{e}_x \cdot \partial/\partial x + \vec{e}_y \cdot \partial/\partial y + \vec{e}_z \cdot \partial/\partial z$	
∇^2	$\nabla \cdot \nabla$	
sinh	$(e^x - e^{-x})/2$	
cosh	$(e^x + e^{-x})/2$	
tanh	$(e^x - e^{-x})/(e^x + e^{-x})$	
arctanh	$\tanh^{-1} \equiv$ invtanh	

1. Introduction

Protons play a crucial role in many bioenergetic processes. In view of Mitchell's chemiosmotic coupling theory, primary proton pumps, such as those linked to electron-transport chains and photosynthetic reaction centers, transfer protons from one side of an insulating closed membrane to the other side, thereby generating both an electrical potential difference ($\Delta\psi$) and pH difference (ΔpH) between the adjacent bulk water phases [1–5]. Together, these two thermodynamic forces ($\Delta\psi$ and ΔpH) constitute the increase of Gibbs free energy (∂G) stored in the system due to the proton translocation ($\partial\vec{H}$, which represents the mole number of transferred protons). This increase has been called the 'proton-motive force' ($\Delta\tilde{\mu}_H$):

$$-\frac{\partial G}{(\partial\vec{H})} \overset{\text{def}}{=} \Delta\tilde{\mu}_H = \tilde{\mu}_H^{in} - \tilde{\mu}_H^{out}$$

$$= F\cdot\Delta\psi - 2.3RT\cdot\Delta\text{pH} \quad [\text{kJ/mol}] \quad (1)$$

(Symbols and their meanings are listed in the glossary, p. 113). This $\Delta\tilde{\mu}_H$, in turn, can be used to drive free energy demanding processes catalyzed by secondary proton pumps, such as phosphorylation of ADP to ATP, active transport and locomotion [2,4].

Though chemiosmotic theory is very popular today, it is not immune to criticism (for recent reviews, see refs. 5–7). One of the moot questions is whether the bulk-to-bulk $\Delta\tilde{\mu}_H$ is the sole communication between primary and secondary proton pumps. Thus, several experimental observations have been discussed in terms of local proton pathways (e.g.; ref. 5), direct collisions between the proton pumps [7,8], conformational coupling [9,10], and redox effects [11].

What forces act on a proton (i.e., a positively charged particle) that is pumped across a membrane, thereby leaving a negatively charged OH^- molecule behind? On the one hand, one would expect that attractive electrical forces acting on the H^+ and OH^- molecule would keep them close to the membrane surface. On the other, pumped protons and the OH^- molecules that are left behind will also tend to equilibrate with the adjacent bulk solutions. Finally, dipoles inside and in the vicinity of the membrane, as well as membrane proteins that may become polarized, might further complicate the situation.

Some of these issues were raised in the discussion between Williams and Mitchell about the so-called 'Pacific-Ocean' effect [12,13]. Williams argued that if charges are 'thrown out into the bulk-solution', as in osmotic theories, this would lead to a dissipation of the bulk-to-bulk $\Delta\psi$, particularly if one of the bulk solutions were the Pacific Ocean. However, Mitchell contended that the electrical capacitance of the lipid membrane is practicably independent of the volume of the outer phase, so that the $\Delta\psi$ component of $\Delta\tilde{\mu}_H$ increases rapidly 'as charge is thrown out into the medium' even if the outer medium is the Pacific Ocean [13].

Earlier, Mitchell noted that due to the high dielectric constant of water ($\epsilon_w = 80$) as opposed to that of the membrane ($\epsilon_m = 2$–3), most of the bulk-to-bulk potential difference would exist across the membrane [3]. Secondly, ψ profiles in the aqueous phase would be of little interest since these would be compensated by pH profiles, the total electrochemical potential, $\tilde{\mu}_H$, being the same throughout each aqueous phase [3]. Finally, according to Gauss' law, the voltage drop across a planar metallic electrical capacitor is only determined by the total amount of transferred charges, irrespective of where they reside in the adjacent conductive phases (e.g., ref. 14).

It has been reported repeatedly that upon energization of energy-transducing membranes (bacterial cells, mitochondria) with a limited amount of oxygen (an O_2 pulse), in the absence of membrane-permeable ions such as K^+-valinomycin and SCN^-, firstly the rate at which O_2 is reduced exceeds the rate at which protons appear in the bulk solution and secondly, the H^+/O ratio is submaximal (refs. 16–19, and McKenzie et al., personal communication). Scholes and Mitchell [15] argued that these observations were due to the low membrane capacitance which accounted for the generation of a high $\Delta\psi$ even at small O_2 pulses, since only 1 nmol H^+/mg protein (i.e., a few turnovers of the electron-transfer chain) need to be pumped across the mitochondrial membrane to raise the $\Delta\psi$ to 250 mV [3]. This would inhibit

further net H^+ transfer as other protons would leak back through the membrane [20]. This was confirmed by the observation that in the presence of permeant ions that abolish $\Delta\psi$ at sufficient concentration, the kinetic discrepancy vanishes and also the H^+/O ratio rises to higher values. However, submaximal H^+/O ratios turned out to be independent of the magnitude of the O_2 pulse and persisted when $\Delta\psi$ was calculated to be energetically insignificant [17,18]. This was recently confirmed by Conover and Azzone (personal communication), who also claimed that submaximal H^+/O ratios are already found at low $\Delta\psi$ values as indicated by the $\Delta\psi$ probe merocyanin 540. Additionally, the H^+/O ratio turned out to increase at higher ionic strengths of the medium (Conover and Azzone, personal communication).

It has been argued that these results were indicative of local proton pathways (ref. 18, and Conover and Azzone, personal communication). For instance, protons would be pumped into small domains close to the membrane, which are connected to one, or a few primary and secondary proton pumps. Therefore, the local $\Delta\tilde{\mu}_H$ could be significantly higher than the bulk-to-bulk $\Delta\tilde{\mu}_H$. Such a 'coupling unit' model for proton-linked free-energy transduction could explain several other anomalies of 'delocalized' chemiosmotic coupling as well [5,6,21,22].

Proton barriers have also been suggested in studies of bacteriorhodopsin. Thus, in the photocycle of this light-driven proton pump of *Halobacterium halobium* (for a review, see ref. 23), it has been observed that protons appear in the bulk aqueous solutions some 4–5 ms after deprotonation of the Schiff base, that is alleged to be involved in the proton-pumping mechanism. This is much later than one would expect from proton diffusion rates (see, however, refs. 5, 25 and 26). Also, these studies have been explained as being indicative of a barrier between a membrane-linked proton pool and bulk solution [26].

These delayed and/or non-appearances of protons are, however, reminiscent of the previously mentioned consideration that electrical forces may tend to keep pumped protons close to the membrane surface. Therefore, we wondered whether the results of these O_2-pulse experiments and bacteriorhodopsin studies could also be explained as electrostatic effects within the context of a chemiosmotic coupling scheme that would allow rapid diffusion of protons between the aqueous bulk phase and the membrane surface.

The exact voltage profile and charge distribution close to a membrane surface are defined by the Poisson-Boltzmann equation [14]. This equation has been solved for many aqueous electrostatic problems in which the condition of electroneutrality was met (or circumvented, e.g., ref. 27) on either side of the membrane, such as ion distributions in the electrical double layer near fixed charges on a membrane surface (Gouy-Chapman equilibria) or ion distributions around fixed charges inside a membrane (Donnan equilibria) (e.g., ref. 28). By contrast, in the studies presented in this paper, which concern a $\Delta\psi$ generated by ion (proton) pumping across a membrane, we are dealing with a membrane with on both sides aqueous solutions, one of which has excess of negative freely moving charge carriers, whilst the other has extra positive charges. This non-electroneutrality in both phases is responsible for an electric field inside the membrane and concomitant potential difference between two bulk solutions. (In none of our calculations do we consider fixed charges.) The case where the membrane was bordered by homogeneous simple salt solutions has been treated by Läuger et al [29]. Using the Poisson-Boltzmann equation, the authors showed that in the presence of a membrane potential, a small amount of ions, representing the excess charge, would accumulate near the membrane in a film with a thickness of approximately the Debye-Hückel length (see also ref. 30). It followed that at low ionic strength, i.e. when the Debye-Hückel length is relatively large, the membrane capacitance depends on the ionic strength. Good agreement between theory and experiment was found [29,31,32].

With the advance of knowledge about the structure of free-energy transducing membranes and their immediate environments [33–37], it has become apparent that the aqueous phases bordering these membranes may not be properly modelled as just highly conductive phases comparable

to electric plates: they contain more than a single charge carrier, as well as high concentrations of proteins and other proton buffers. Consequently, it seemed appropriate to calculate the expected spatial redistribution of ions upon energization of biologically realistic membranes. The results would allow up-to-date answers to the questions raised above and in discussions of the Pacific-Ocean effect.

In this paper, we report the results of such calculations. Various geometries (planar symmetry, an array of closely stacked parallel membranes and the vesicle), the presence of pH buffers in the aqueous phases and the presence of proteins adjacent to the membrane core are considered. We show that only in the latter two cases might pumped protons be held close to the membrane surface and remain undetected by bulk-phase probing methods.

2. Results

To simplify the calculations and the discussion of their results we consider a simplified picture of a biological membrane. The membrane core is considered to be a homogeneous, hydrophobic phase devoid of charges with a relative dielectric constant of 2 and a thickness of 4 nm [29]. In two of our three models it is bordered on either side by a homogeneous aqueous solution containing a monovalent salt and/or a simple pH buffer. In the third model, there are additional protein layers (with properties specified below) between homogeneous aqueous solutions and the membrane. In all models, diffusion of protons and other solutes between the membrane surface and the aqueous bulk phases is unhindered.

We shall be discussing the situation after a net translocation of protons across the membrane has taken place (as a result of proton pumping exceeding proton back leakage). This may represent the situation at any point during an O_2-pulse experiment, or in a steady-state situation where proton pumping and proton back leakage compensate each other (here kinetic arguments given in ref. 26 would not apply). Again for simplicity, we always assume the membrane core to be impermeable for ions other than protons.

The ways by which we calculate the equilibrium profiles of the electric potential, ψ, and concomitant ion distributions upon proton pumping are described in the appendices. Appendix A reviews the method developed by Läuger et al. [29] for an infinite planar membrane devoid of fixed charges bordered by simple salt solutions. Appendix B gives an adjustment to this method for the presence of buffers in the aqueous phases. Appendix C shows how the profiles can be calculated in the presence of a protein layer bordering the membrane. In appendix D we treat an array of planar membranes and in appendix E we evaluate a spherical vesicle. The technique for all cases is similar: the profile of ψ is evaluated by solving the Poisson-Boltzmann equation using appropriate boundary conditions. Subsequently the concentration profiles of all ions are calculated by inserting the solution of $\psi(x)$ into the Boltzmann equation of every ion species.

2.1. Charge redistribution near a planar membrane bordered by salt solutions

The full lines in fig 1 review the profile of $\psi(x)$ (x-axis is taken perpendicular to the membrane) at low ionic strength (1 mM KCl, traces designated a) and at physiological ionic strength (150 mM KCl, traces with b). The effect of ions on the relative dielectric constant of water (ϵ_w) was corrected for by using $\epsilon_w = \epsilon_w^o + \delta \cdot \Sigma\, c_i$, where ϵ_w^o ($= 80$) is the ϵ_r of pure water (25 °C) [38]. For a KCl solution, δ equals -11 [38]. These corrections, however, usually amount to less than 2%. The charge density ρ ($= F \cdot (H^+ + K^+ - Cl^- - OH^-)$) as a function of x is depicted by the dashed lines. In the two calculations the same amount of charge was considered to have been translocated across the membrane. In fig. 1, we see that at low ionic strength (1 mM KCl), the bulk-to-bulk $\Delta\psi = \psi(\infty) - \psi(-\infty) = 200$ mV, is significantly higher than the transmembrane potential difference $\Delta\psi_m = \psi(r_m) - \psi(-r_m) = 178$ mV. At even lower ionic strength, this effect becomes much more pronounced (not shown) (cf. ref. 29, p. 39). This is due to the effect of the negative charge

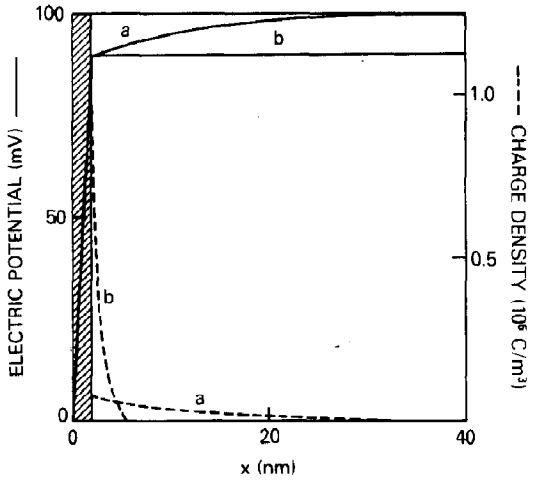

Fig. 1. Electric potential (———) and charge density (------) profiles generated by a fixed amount of charge separation across a membrane. (Case a) 1 mM ionic strength, (Case b) 150 mM ionic strength. $x = 0$ refers to the middle of the membrane; $x = 2$ represents the membrane-water transition. $\epsilon_m = 2.0$, $\epsilon_w = 80.0$, $d_m = 4.0$ nm.

left on the other side of the membrane. The dashed line (a) in fig. 1 shows that even at low ionic strength, the excess charge accumulates close to the membrane surface. At locations beyond 40 nm off the surface, the solution becomes nearly electroneutral ($\rho \to 0$). The total amount of accumulated charge per membrane surface area ($\sigma = \int_{r_m}^{\infty} \rho \cdot dx$) equals the area underneath the dashed lines. This turns out to be 0.790×10^{-3} C/m^2. Thus, a membrane capacitance, based on the bulk-to-bulk $\Delta\psi$ (as we shall usually do in the following), $C = \sigma/\Delta\psi$ of 0.395 μF/cm^2 was calculated (cf. ref. 29). Furthermore, fig. 1 shows that under physiological circumstances (150 mM KCl, lines b), the potential drop between the membrane surface and bulk solution becomes extremely small. Nonetheless, all excess charges still reside in the small region of the potential drop. In this case, the $\Delta\psi_m$ is the same as that in the situation of low ionic strength. However, a smaller $\Delta\psi$ is generated ($\Delta\psi \approx \Delta\psi_m = 178$ mV). The total charge/surface area now turns out to be again 0.790×10^{-3} C/m^2, and the membrane capacitance amounts to 0.438 μF/cm^2.

2.2. Effect of polarizability of the medium surrounding the membrane on the position of the charge

Fig. 2 shows the ρ and ψ vs. x profiles if at physiological ionic strength the polarizability of the medium surrounding the membrane were, fictively, $5000\epsilon_0$. By comparison with fig. 1b, this illustrates that higher polarizability of the conducting phase indeed enables the free charge to penetrate more deeply into the bulk phase. However, the effective charge, i.e., $\rho + \rho_{pol}$, where ρ_{pol} refers to the charge density due to dipole polarization, remains very close to the membrane. If the aqueous medium were infinitely polarizable, all excess free charges would spread out completely through the entire bulk phase, with the effective charge still remaining exceedingly close to the membrane.

Mitchell [3] argued that, although the conveyed charges smear out equally over the bulk phase, the high polarizability of water still results in $\Delta\psi$ being only slightly larger than $\Delta\psi_m$. We see that this would be correct, i.e., the charges would be ejected into the medium for some 20 nm, if the permittivity of water were very high, say, over 5000. In reality, ϵ_w^o is only 80, being insufficient to have the translocated charge spread further than 4 nm.

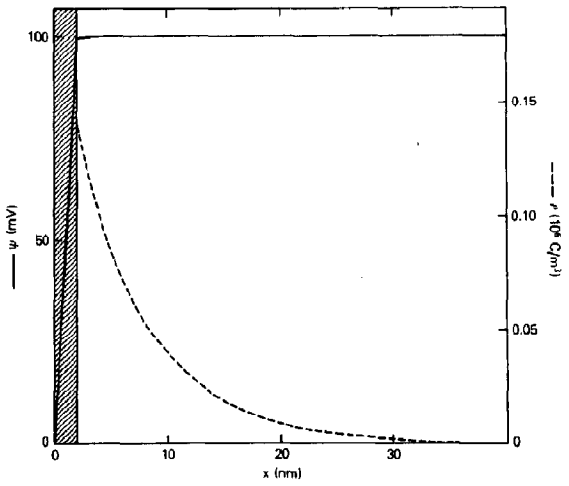

Fig. 2. $\psi(x)$ (———) and $\rho(x)$ (------) profile upon proton pumping across a membrane into a medium with high polarizability. $\epsilon_m = 2.0$, $\epsilon_{medium} = 5000$, $d_m = 4.0$ nm.

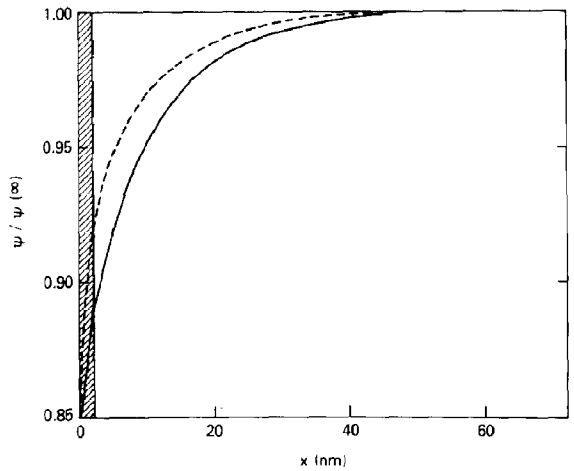

Fig. 3. Profile of normalized electric potential $\psi(x)/\psi(\infty)$ at different bulk-to-bulk $\Delta\psi$. (———) $\Delta\psi = 20$ or 200 mV; (------) $\Delta\psi = 2$ V. Low ionic strength (10^{-3} M KCl). $\epsilon_m = 2.0$, $\epsilon_w = 80.0$, $d_m = 4.0$ nm.

2.3. Effect of variation of $\Delta\psi$

Fig. 3 shows the (normalized, i.e. $\psi(x)/\psi(\infty)$) ψ vs. x profiles at low ionic strength (10^{-3} M KCl), if the respective bulk-to-bulk potential differences were 20 mV, 200 mV (both represented by the full line) and 2 V (dashed line), as calculated from the non-linear Poisson-Boltzmann equation. The profiles differ significantly for membrane potential differences over 200 mV. Application of Boltzmann's equation to calculate the concomitant ρ profiles and total amount of accumulated charges yields membrane capacitances of 0.395, 0.395 and 0.408 μF/cm^2 respectively. This $\Delta\psi$ dependence of C vanishes at higher ionic strength.

2.4. Where are the protons?

Which particles represent the excess surface charges, protons or salt ions? Are the originally pumped protons restrained from dissolving into the bulk phase by electrical forces? This question can be addressed conveniently by use of the Boltzmann equation, which applies to all mobile particle species. For protons, and for any $x > r_m$:

$$H^+(x) = H^+(\infty) \cdot \exp(-q_e \cdot (\psi(x) - \psi(\infty))/kT) \quad (2)$$

For K^+:

$$K^+(x) = K^+(\infty) \cdot \exp(-q_e \cdot (\psi(x) - \psi(\infty)))/kT \quad (3)$$

Therefore, at pH 7 and 1 mM KCl

$$H^+(x)/K^+(x) = H^+(\infty)/K^+(\infty) = 10^{-7}/0.001 = 10^{-4} \quad (4)$$

We note that at pH 7, the accumulated charges are mainly represented by salt ions, even at low ionic strength (1 mM KCl). This leads us to the conclusion that unless the proton concentration in the medium approaches the ionic strength (for such cases, see sections 2.6 and 2.7), the originally pumped protons are displaced by salt ions, and readily diffuse into the bulk solution, the (free) surface charge density being maintained.

2.5. Different geometries

2.5.1. Parallel membranes

We have also calculated the profile of the electric potential for an array of (an infinite number of) parallel membranes (cf. fig. 4, three out of the array are shown as the hatched areas). Such a calculation might be appropriate for the highly folded inner mitochondrial membrane, or the stacked thylakoid membranes in chloroplasts. The mathematical model for this situation is outlined in appendix D. The full line in fig. 4 shows how, at an intermembrane spacing of $2l = 3$ nm, $d_m = 3$ nm, and a 100 mM KCl solution (with reduced polarizability) between the membranes, the electric potential varies with the position in space. The details of this variation differ from those in the case of the single planar membrane (fig. 1), mainly because now the electric field must become zero at a distance l from the membrane, rather than at infinity. In either system, however, the difference in electric potential between the membrane surface and the positions farthest away from the membrane is small: a few percent of the transmembrane electric potential $\Delta\psi_m$. It is important to remember that our model membrane is devoid of surface charge in order to stress the effects of charge translocation. The presence of surface

charge has recently been shown to have strong implications, especially in the case of closely stacked membranes [40].

At low ionic strength, however, the plane parallel case differs strongly from the case of a single membrane in that the voltage increase in going from the membrane surface to the bulk phase (defined as halfway between the membranes) does not become very high. Thus, it was calculated that at an intermembrane spacing of 8 nm, this potential difference never exceeds 25 mV if the transmembrane potential equals 200 mV. By contrast, in the case of a single membrane, at very low ionic strength (i.e., < 1 mM), most of the bulk-to-bulk $\Delta\psi$ exists between the membrane surface and the bulk solution. Furthermore, at extremely close stacking of the membranes, it was evaluated that the potential difference between the membrane surface and halfway between the membranes becomes a fraction of the transmembrane potential difference that is independent of the ionic strength, as shown in fig. 5. This occurs as the Debye-Hückel length ($1/\kappa$) exceeds the intermembrane spacing; then medium polarization due to ion movement becomes inconsequential. In physiological circumstances, $1/\kappa$ is equal to about 1 nm. Thus at certain metabolic states [24,36,40–42], the stacking of the membranes in mitochondria and chloroplasts could indeed be of the same order of magnitude as $1/\kappa$. As the intermembrane spacing becomes wider and wider, the behaviour of the systems converges to that of a single membrane and exhibits the ionic strength dependence of that case (fig. 5). The dashed line in fig. 4 shows that, even at physiological ionic strength, the charge pumped across the membranes extends over a significant part of the intermembrane space (cf. ref. 40).

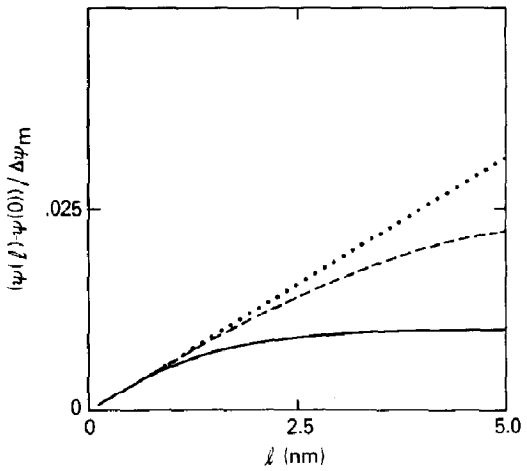

Fig. 5. Relative potential difference between the center of an aqueous phase in fig. 4 ($x = 0$) and the membrane surface ($x = l$) (i.e., $(\psi(l)-\psi(0))/\Delta\psi_m$) as a function of the intermembrane spacing l. At very close stacking, i.e., when $(1/\kappa) > l$, the potential drop becomes independent of the ionic strength. (———) 150 mM KCl; (- - - - -) 20 mM KCl; (· · · · · ·) 1 μM KCl. Calculated as described in appendix D.

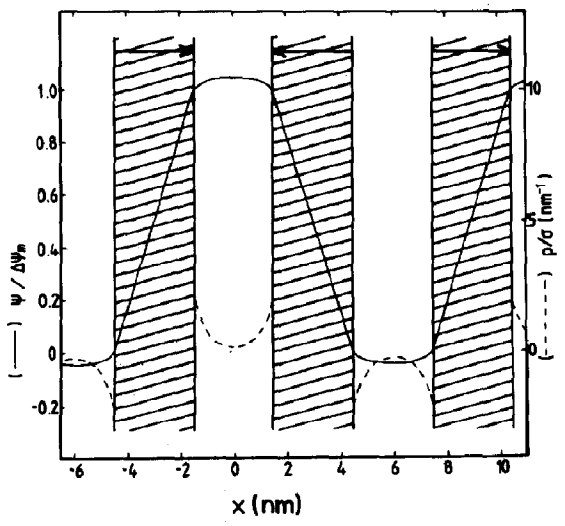

Fig. 4. Model of an array of infinite membranes. (———) Profile of ψ upon charge separation across the membranes. (- - - - - -) Charge density. Arrows indicate the direction of H^+ pumping. For further explanation, see text. Calculations for $d_m = 3$ nm, $l = 1.5$ nm, $\epsilon_m = 6$, $\epsilon_w = 20$, 100 mM KCl solution.

2.5.2. *Spherical geometry*

We have also considered the (idealized) spherical membrane vesicle (cf. appendix E). The membrane potential profiles do not deviate much from those of the planar case, unless the radius of the vesicle were to be of the same order of magnitude as the thickness of the membrane. This is not realistic for vesicles of biological membranes. The capacitance per unit surface is found to be independent of the size of the vesicle, if the surface of the vesicle is calculated based on the average of the two radii of the vesicle.

2.6. Buffered media

In the calculations presented up to this point, aqueous media were considered to consist of solutions of KCl in water near physiological pH values. Thus, the total proton concentration would be equal to the concentration of free protons which, at pH 7, would be much smaller than the concentration of K^+. Physiological media however include (H^+) buffers, such that the total H^+ concentration (i.e., that including the protons bound to the buffer) would be much higher than 10^{-7} M and could actually approach the concentration of the buffer. We investigated whether in such cases the charge accumulation near the membrane surface arising upon proton pumping might consist largely of buffer-bound protons rather than salt cations.

The problem becomes particularly simple when one considers at a fixed ionic strength the replacement of part of the KCl with buffers A and B (with pK_a values ≈ 7; cf. appendix B). Such a substitution does not affect the Debye-Hückel length $1/\kappa$. Consequently, the profile of the electric potential is identical to the full line labeled b in fig. 1.

The corresponding dashed line still gives the charge density. However, part of this charge density now consists of protons bound to the buffer. In analogy to the derivation of eq. 4, the ratio between total (i.e., free plus buffer-bound) H^+ and K^+ at any point in space is given by:

$$(H^+(x) + AH^+(x))/K^+(x) = (H^+(\infty) + AH^+(\infty))/K^+(\infty) \quad (5)$$

In the case where AH^+ and K^+ were equal (such a situation would be approximated by a solution of 50 mM KCl and 75 mM Tris (Cl) at pH 7.8), 50% of the charge accumulated near the membrane would consist of protons bound to the buffer. Consequently, 50% of the translocated protons would go undetected by a pH electrode located in the bulk phase. Conversely, whenever the salt concentration exceeds the concentration of the buffer by a factor of 10 or more and if the membrane surface is readily accessible to the salt, one would expect all (> 90% of) the pumped protons to migrate rapidly to the bulk phase.

2.7. Additional protein layer

In section 2.6 we analyzed the situation in which a proton buffer occurred everywhere in the aqueous medium. Aqueous phases do not always have high average concentrations of proton buffers. In some cases, it may be more realistic to assume that in a region close to the membrane there is a rather high buffer concentration. We studied a model where the buffer consists of proteins associated with the membrane. (fig. 6; appendix C) This case corresponds to that in section 2.6 except that the H^+ buffer is now limited to a region close to the membrane. Furthermore, it was assumed that the salt cation (K^+) may not partition equally between the protein and water phases, as expressed by the equilibrium partition coefficient $\Pi_K = ([K^+]_p/[K^+]_w)$ (in the case of $\psi_p = \psi_w$).

Fig. 7 shows ψ (full line) and $H^+(x) - OH^-(x)$ (dashed line) as well as $K^+(x) - Cl^-(x)$ (dotted line) profiles for the case where we consider such a protein layer adjacent to the membrane surface according to the model outlined in fig. 6. In the calculation leading to fig. 7, we assumed the thickness of the protein layer to be 13 nm [43], and further: a relative dielectric constant (excluding the Kirkwood-Shumaker polarization [44]) for the protein (ϵ_p) of 10, buffering groups present at

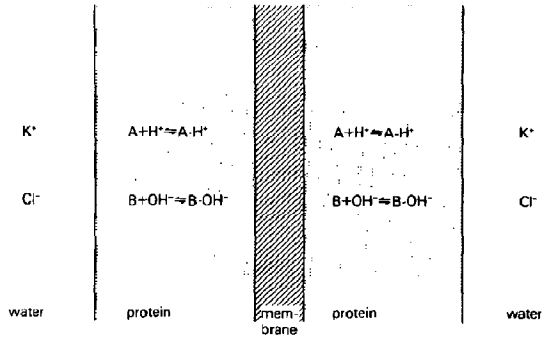

Fig. 6. Model of a five phase system comprising two aqueous solutions separated by a biological membrane with two protein layers, one on each side of it. For further explanation, see text and appendix C.

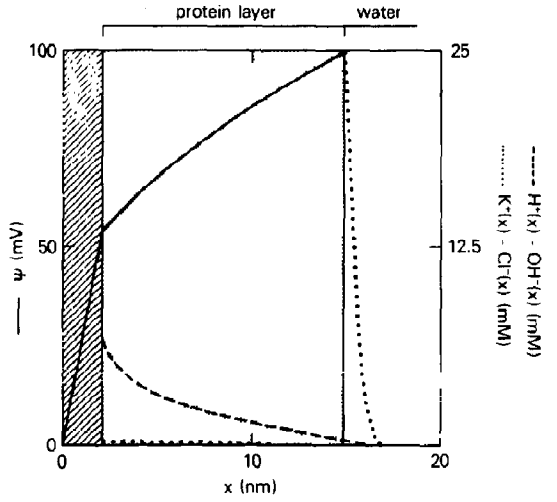

Fig. 7. Profile of ψ (———) and charge density as represented by excess protons (------) and excess salt ions (·····) in the presence of a membrane potential, if a salt-impermeable protein layer of 13 nm thickness borders the membrane. 150 mM KCl; buffer concentration, A = B = 100 mM; $\Pi_K = 10^{-4}$; pH 7.0; $\epsilon_m = 2.0$, $\epsilon_p = 10.0$; $pK_a = 5$.

concentrations of 1 mM in the AH^+ and $B\text{-}OH^-$ and 100 mM in the A and B forms. The partition coefficient (Π) for K^+ and Cl^- between water and the protein phase was chosen to be 10^{-4}. [KCl] = 150 mM in the bulk phase. For simplicity the water phase outside the protein layer was considered to be devoid of buffer. Interestingly, there is a significant decrease in ψ in the protein layer, and a tiny drop in ψ for the aqueous phase. Furthermore, we see that the charge density inside the protein layer is mainly represented by excess protons.

The total fraction of pumped protons that is held inside the protein layer can be evaluated as follows: The amount of excess charge inside the protein layer (σ_p) equals:

$$\sigma_p = \int_{r_m}^{r_p} (\rho^+(x) - \rho^-(x))\, dx \quad [C/m^2] \qquad (6)$$

Thus, σ_p can be calculated by combining eqs. C2, C3, C5 and C7, and integrating over x. The relative contributions of protons (σ^H) and salt ions (σ^K) to σ_p can be evaluated from the corresponding Boltzmann equations. For the example of fig. 7:

$$\frac{\sigma^H}{\sigma^K} = \frac{H^+(x) + H^+(x)\cdot A/K_a}{K^+(x)}$$

$$= \frac{H^+(\infty) + H^+(\infty)\cdot A/K_a}{\Pi_K \cdot K^+(\infty)} = 66.7 \qquad (7)$$

The total amount of charge (σ) residing in the protein layer plus water phase equals: $\sigma = \epsilon_m \epsilon_0 \cdot \Delta\psi_m / 2r_m$. Now the fraction $\sigma^H/\sigma = \sigma^H \cdot \sigma_p/(\sigma^H + \sigma^K)$ can be calculated. This fraction represents the amount of pumped protons that are held inside the protein layer. The result of these calculations was that σ^H/σ was 43% (the rest of σ is represented by salt ions near the protein-water interphase, see fig. 7).

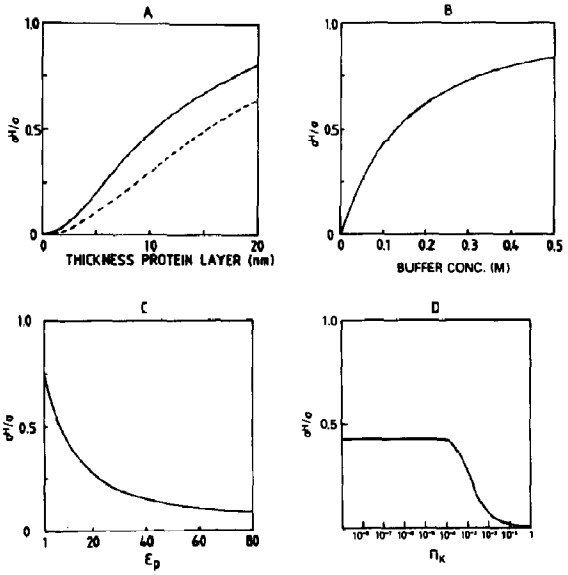

Fig. 8. Fraction of excess protons (σ^H) inside the protein layer contributing to the total amount of excess charge (σ) at different properties of the protein bordering the membrane. $\epsilon_m = 2.0$, pH 7.0, 150 mM KCl, $r_m = 2$ nm. (A) Variation of r_p; $\epsilon_p = 10.0$, $\Pi_K = 10^{-4}$; (———) buffer concentration, 200 mM; (------) buffer concentration, 100 mM. (B) Variation of buffer concentration; $\epsilon_p = 10.0$, $r_p = 15$ nm, $\Pi_K = 10^{-4}$. (C) Variation of ϵ_p; $r_p = 15$ nm, buffer concentration, 100 mM, $\Pi_K = 10^{-4}$. (D) Variation of Π_K; $\epsilon_p = 10.0$, $r_p = 15$ nm, buffer concentration, 100 mM.

Variation of σ and ϵ_m had little effect upon the magnitude of this fraction. However, if the buffer concentration was lowered to 10 mM, the thickness of the protein layer was less than 4 nm, or particularly if Π_K was chosen to be higher than 10^{-4}, the fraction dropped sharply (fig. 8), σ^K increased significantly up to the total σ, and the ψ profile approached that of the situation where no protein layer was present. In contrast, variation of ϵ_p showed some interesting features. It turned out that if ϵ_p was lower than 10, σ^H/σ rose significantly above 0.5 (fig. 8C).

3. Discussion

The exact profile of ψ is important for a number of reasons: First, the interpretation of ψ measurements depends on it [40]. $\Delta\psi$ is often measured by 'surface' or 'bulk' probes, which are often found to yield different results [6]. Bulk probes are membrane-permeant ions which redistribute over the two compartments separated by the membrane in response to changes in the bulk-to-bulk $\Delta\psi$, so that the electrochemical potential ($\tilde{\mu}_i = F\psi - RT \ln c_i$) remains the same in both compartments. Surface probes are dyes, the spectroscopic properties of which respond to changes in the electric field. Thus, the question concerns where these dyes dissolve in the membrane, and how the electric field at the location of the probe is related to the $\Delta\psi$ (R.J. McKenzie, L. Faulk, G.F. Azzone and T.E. Conover, personal communication), and if this relation is the same under calibration and measurement conditions.

Second, although in the delocalized coupling model (i.e., with infinite proton conductance in either aqueous phase) $\Delta\tilde{\mu}_H$ would be constant, irrespective of the locations in the two opposite aqueous phases between which it would be measured, its components $\Delta\psi$ and ΔpH may well vary with these locations. For instance, if one were to measure ψ_{in} close to a fixed negative charge in the internal phase and ψ_{out} close to a fixed positive charge in the external phase, the local $\Delta\psi$ would differ from that between locations distant from such fixed charges. This phenomenon can have important implications, as $\Delta\psi$ and ΔpH can well have different kinetic effects on proton pumps [45–48], depending on which transition is most rate limiting.

Summing up the results of this paper, we arrive at the following picture of a water-membrane-water system with a $\Delta\psi$ generated by proton pumping: Pumping of protons across a membrane results in an excess of mobile positive charges at one side of the membrane, and an excess of negative charges at the other. Evaluation by use of the Poisson-Boltzmann equation [29] shows that under physiological circumstances, ψ is almost homogeneous throughout the bulk solutions. (Hence we may say: $\Delta\psi \overset{\text{def}}{=} \Delta\psi_b \approx \Delta\psi_m$.) However, there is a tiny drop in ψ in going from the bulk ($x = \infty$) to the membrane surface ($x = r_m$). Although this change is extremely small and close to the surface, this drop represents all excess charge accounting for non-electroneutrality in that area.

$\Delta\psi$ is already formed during the proton translocation from one side of the membrane to the other and we see that charge, once it has been translocated through the isolating membrane, does not become delocalized ('osmotic'), but will accumulate near the membrane surface according to a Boltzmann distribution. Therefore, pumped protons can only dissolve into the bulk phase provided other ions (e.g., salt ions) compensate, the surface charges being preserved [49]. At any reasonable ionic strength, this is expected to take place readily. Thus, this may clarify one point of the Pacific Ocean discussion: the charge does not delocalize, but the pumped protons do. Another point of that discussion referred to concern about the possible dissipation of the electric field inside the membrane if the excess charge were to disappear into the medium [12]. Even if the charge penetrated into the medium, the electric field inside the membrane would not be affected as it depends solely upon the magnitude of the charge separation, irrespective of the location of the excess charge relative to the membrane (see also fig. 1).

At apparent variance with the conclusion that all the pumped protons dissolve readily into the bulk phase are experimental observations of pH changes in the bulk phase upon low-level energiza-

tion of free-energy transducing membranes. As reviewed in section 1, the pH changes tend to be smaller than expected from the known total amount of pumped protons. Myatt and Jackson [50] argued that this non-appearance of protons might be due to incomplete electron-chain turnovers between subsequent light flashes that energized their chromatophores of *Rhodopseudomonas capsulata*. This explanation does not apply to O_2-pulse experiments where the amount of a single addition of oxygen is always completely consumed.

The observation that even at low electric potential differences between the aqueous bulk phases not all translocated protons appear in the bulk phase can be (and has been; for a review, see ref. 5) explained if there were to be a resistance to proton movement between the membrane surface and the aqueous bulk phase plus a back leakage pathway between the two aqueous bulk phases [51]. Junge and Polle [24] explained the non-appearance of protons in the bulk phase through a kinetic retardation of proton diffusion alone, due to a high concentration of immobile buffers. As detailed elsewhere [25], such an explanation only works in the kinetic sense and does not explain non-appearance on time scales allowing proton equilibration with the bulk phase. In this paper, we came upon two sets of circumstances under which the net number of protons appearing in the bulk phase was lower than the number of protons translocated across the membrane even though proton diffusion was assumed to be completely unhindered. One set of circumstances involved proton buffers constituting a major fraction of the medium ionic strength. Then the pumped protons rather than exchange with the bulk-phase salt cation would exchange with the bulk-phase protonated buffer molecules. (This exchange need not necessarily consist of actual movement of a protonated buffer molecule and reverse movement of an unprotonated buffer molecule, but might also boil down to hopping of protons between buffer groups). In this situation, there would be a net confinement of protons to the region near the membrane surface.

We also investigated another possibility in which such non-appearance of protons in the bulk phase would be a purely electrostatic effect. We considered an additional protein layer adjacent to the membrane surface. The presence of something like such a layer seems feasible on the basis of the high protein/lipid concentration ratios in biological membranes and the known structures of energy-transducing organelles, particularly mitochondria [34,36,37,43]. We note that, because we modelled the membrane as a 3–4 nm thick hydrophobic core, part of this protein layer would in actual fact correspond to the more hydrophilic regions of the actual membrane. We also assumed unequal distribution of salt ions between the protein and water phase, i.e., $\Pi_K = (K_p^+/K_w^+)_{eq} \ll 1$. This is justified as a protein phase probably does not allow for solvation of large amounts of salt ions. Protons and OH^- molecules, however, are supposed to dissolve easily into the protein layer, since they can reside on protein-hydration water and on ubiquitous buffering groups.

In section 2.7 we discussed a simple model for such a system (figs. 6 and 7; appendix C). We saw that under physiologically realistic circumstances, there would be a significant potential drop inside the protein layer (about 50% of the $\Delta\psi$), and only a tiny drop in the water phase. The H^+/K^+ ratio near the membrane's surface turned out to be much greater than in the absence of a protein layer. Thus, with a protein at a buffer group concentration of 100 mM, $K_a = 10^{-5}$, pH 7, $\Pi_K = 10^{-4}$ and 150 mM salt solution, the $H^+(r_m)/K^+(r_m)$ ratio could be calculated to be 67. This means that in this case, most excess charges inside the protein layer are represented by protons, whereas in the absence of a protein layer it is predominantly salt ions that account for the excess charges near the membrane surface. Also, a significant fraction of the excess charge on the positive side of the membrane would actually reside in the protein layer. Thus, due to the presence of a salt-impermeant, hardly polarizable, protein layer, which causes lowering of the ionic strength nearby the membrane, part of the pumped protons can be held inside that layer. There is some controversy in the literature concerning the polarizability of proteins. Different theoretical studies report values of ϵ_p varying between 1 and 15 [38,53,54]. Our ϵ_p value reflects the protein

polarizability exclusive of the Kirkwood-Shumaker [44] proton polarization and may therefore be significantly lower than overall values reported for ϵ_p [38].

Consequently, we contend that if such a protein layer were present, or if the medium (in the vicinity of the membrane) were to consist largely of buffer, the non-appearance of protons in the bulk phase could be fully explained as an electrostatic effect. Indeed, our simple model can explain the observed results of O_2-pulse experiments. The σ^H/σ ratio represents the amount of pumped protons that are not measured in the bulk phase upon energization. Thus, $1 - \sigma^H/\sigma$ is proportional to the measured H^+/O ratio. The above-mentioned calculations of σ^H/σ show that only a fraction of the originally pumped protons are exchanged with K^+, enabling the protons to dissolve into the bulk aqueous solution. Therefore, only substoichiometric H^+/O ratios will be measured upon energization. In addition, this H^+/O ratio is expected to be independent of the size of the O_2 pulse, because the magnitude of σ had little effect upon the σ^H/σ fraction.

Furthermore, as one can infer from eq. 7, σ^H/σ^K decreases at higher salt concentration which then implies that σ^H/σ also decreases, so that we can explain why the measured H^+/O ratio may increase at higher salt concentration, as found by Conover and Azzone (personal communication).

In the case of the protein layer, the kinetic discrepancy between oxygen consumption and proton appearance in the bulk solution could also be explained. If indeed K^+ were to diffuse with difficulty into the protein layer, it would take some time to arrive at the equilibrium H^+/K^+ ratio in the protein layer after protons have been pumped into the layer. In the presence of SCN^- or of K^+-valinomycin, ions can permeate into the protein layer and both phenomena will disappear, even before $\Delta\psi$ has been dissipated.

Also, in the matter of retarded proton appearance upon deprotonation of the Schiff base in the photocycle of bacteriorhodopsin, we must bear in mind that pumped protons can only dissolve in the bulk solution, provided other ions compensate, either by dissipating the generated (local) $\Delta\psi$ or by replacing accumulated protons near the membrane surface.

In the explanation of the lack of bulk-phase observable protons in oxygen-pulse experiments, the model calculations for the case where the aqueous medium largely consisted of protonatable molecules might seem less relevant than calculations for the situation with the salt-impermeant protein layer. We would suggest, however, that the actual situation might be intermediate between the two model situations. Considering the intermembrane, extramatrix space in mitochondria (the periplasmic space in bacteria), we note high protein concentrations and hence high buffer capacities which extend over tens of nanometers. If these spaces were salt-permeable, this would come close to the model with ready accessibility of the membrane surface for salt cations and a high buffer content of the media (section 2.5). For the mitochondrial matrix space this is true a fortiori. Although the mitochondrial matrix contains about 100 mM K^+, the anions are largely protonatable substances (proteins, adenine nucleotides, phosphates). Mitchell and Moyle [52] estimated the buffer capacity of the intramitochondrial matrix at approx. 20 mM H^+/pH unit. This would correspond to the presence of a buffer with a pK_a value of 5 at a concentration of 2 M. In most of our calculations we assumed a buffer concentration of only about 100 mM. We conclude that consideration of the effects revealed by our calculations is important in discussing proton pumping across actual free-energy transducing membranes.

Note that in these explanations the electrochemical potential of both protons and salt ions is the same throughout the protein and water phases on either side of the membrane. This is an important feature, since it is a more reasonable assumption that proteins are nearly impermeable for salt ions (or that the space bordering membranes contains buffer rather than nonprotonatable salts), than considering a proton diffusion barrier between a local proton pool and bulk solution (as is usually done in localized chemiosmotic coupling schemes; for a review, see ref. 5): particularly protons are exceedingly mobile in aqueous and most protein phases. We would like to emphasize,

however, that there remain several anomalies of the delocalized chemiosmotic coupling scheme that have not as yet been explained by solely assuming the presence of a buffer-rich or salt-impermeable protein layer, bordering the membrane.

The potential profile inside the protein layer (fig. 7) might have additional implications. Firstly, if the kinetics of $\vec{H}^+$-ATPase depend on $\Delta\psi$ and ΔpH in different ways, then the crucial question is where the active part of the $\vec{H}^+$-ATPase resides inside the protein layer. Secondly, fluctuations of the relative contributions of $\Delta\psi$ and ΔpH to the $\Delta\tilde{\mu}_H$, due to the presence of a salt-impermeable protein layer or of local buffers, might be of great interest in the coupling mechanism [55,56]. Thirdly, we infer from fig. 7 that the electrical field varies inside the protein layer. This might be of importance for $\Delta\psi$ measurements with surface probes (cf. ref. 40). For instance, if the probe resides inside the protein layer, it will respond to changes in the ψ profile. Addition of K^+ and valinomycin, which is usually part of the calibration procedure, might make the protein layer more permeable for salt ions. This could affect the ψ profile inside the protein layer considerably. Hence, the response of the probe to a K^+ plus valinomycin induced diffusion potential might be totally different from that to a $\Delta\psi$ generated by proton pumping.

We have tackled several electrostatic problems by use of the Poisson-Boltzmann equation in a manner similar to that carried out in Debye-Hückel and Gouy-Chapman theory. Clearly, in all these cases we are dealing with local non-electroneutrality where ensembles of charged particles are subjected to electrical forces and also tend to even out concentration profiles. In the Poisson-Boltzmann equation we assume all particles to be point charges being dissolved in a dielectric continuum. Since the radius of hydrated ions is only of the order of tenths of a nanometer, and thus smaller than the dimensions of our system (e.g., $d_m = 4$ nm), the assumption of point charges seems to be feasible. The latter assumption also appears to be appropriate: In the absence of excessively strong fields, water, membranes, and proteins behave as linear dielectrics [38,57]. Furthermore, in our calculations we used the non-linear Poisson-Boltzmann equation if the condition $(q_e(\psi(r_m) - \psi(\infty))) \ll kT$ was not fulfilled (except for the case of the protein layers). In classical Debye-Hückel theory, application of the non-linear Poisson-Boltzmann equation leads to inconsistency with the assumption that energy relationships between the central ion and peripheral ions ought to be reciprocal [58]. In our case, as well as in that electric double layers, this problem does not arise because it is the charge separation across the membrane that mainly determines the energy of the charged particles in the vicinity of the membrane [59]. In fact, we neglect Debye-Hückel screening of charge carriers near the membrane surface. Therefore, the distribution of ions in response to the electric field near the membrane is given by the Boltzmann equation.

One could argue that it is improbable that there is a continuous protein layer bordering the phospholipid bilayer and that this assumption implies departure from the conventional Singer model of biological membranes. Studies of energy-coupling membranes, however, have shown that the protein/phospholipid ratio is so high that, at least locally, considerable parts of the membrane enzymes protrude from the membrane [34,35]. For convenience, we assumed the protein layer to be continuous to illustrate some interesting effects. Additionally, one could argue that the buffering groups inside the protein layer are not sufficiently concentrated to apply a continuous model to that layer. Indeed, secondary effects associated with possible complications inherent to the application of the Poisson-Boltzmann equation may detract somewhat from the precise results of our calculations. However, they will not compromise the qualitative essence of our results, namely, the facts: (i) that upon proton pumping, protons need to be exchanged with co-ions in order to dissolve into the bulk solution and (ii) that this exchange might be jeopardized by the presence of mobile buffers or immobile proteins adjacent to the membrane.

Appendix A: Electric potential profile for a single planar membrane surrounded by unbuffered aqueous media

For the sake of completeness, we derive again the profile of ψ across a membrane in the pres-

ence of net charge translocation, following the method of Laüger et al. [29]. Let us consider an infinite planar membrane with a conducting aqueous phase on both sides. We have conveyed net charge (i.e., σ C/m^2) from one side of the membrane to the other. We assume planar symmetry, i.e., the excess charge spreads equally over the surface on either side of the membrane (i.e., ψ and ρ vary only in the x-direction, perpendicular to the membrane surface). In the presence of a membrane potential, caused by a charge separation, electrical forces will tend to keep the excess charge carriers in either aqueous phase close to the membrane. Adversely, the accumulated particles will tend to diffuse off the membrane into the bulk phase, thereby evening out the concentration profile and increasing the entropy of the system. An interesting paradox which is a consequence from Gauss' Law is that if, in this case of planar symmetry (and also for spherical symmetry), the conveyed charge resides further from the membrane, the bulk-to bulk $\Delta\psi$ increases (the symbol $\Delta\psi$ always refers to the bulk-to-bulk potential difference in this paper), but the transmembrane $\Delta\psi_m$ as well as the field inside the membrane, E_m, remain the same, and are fully determined by the magnitude of σ, irrespective of where the charges are! Hence, if charge moves further away from the membrane, this does not lead to dissipation of the $\Delta\psi$, as Williams [12] feared in the Pacific-Ocean discussion.

The above-mentioned competition between electrical and thermodynamic forces will culminate in an equilibrium distribution of the transferred charges, $\rho(x)$, and concomitant profiles of $E(x)$ and $\psi(x)$ which can be evaluated as follows: the electric field is a direct function of the distribution of charges following:

$$\frac{\partial E}{\partial x} = (\rho_{pol} + \rho)/\epsilon_0 \qquad \text{(A1)}$$

Eq. A1 can be simplified according to dielectric theory [14,38,60,61] into:

$$\frac{\partial E}{\partial x} = \rho/(\epsilon_r \epsilon_0) \qquad \text{(A2)}$$

The electric field is also the spatial derivative of the electric potential:

$$E = \frac{-\partial\psi}{\partial x} \qquad \text{(A3)}$$

Combining eqs. A1 and A3 gives Poisson's equation:

$$d^2\psi/dx^2 = -\rho/(\epsilon_r \epsilon_0) \qquad \text{(A4)}$$

which describes the electrostatic interactions between the free point charges in a dielectric continuum.

Since the energy of the charged particles near the membrane surface is mainly determined by the electric field due to the charge separation, Boltzmann's equation reads:

$$c_i(x) = c_i(\infty) \cdot \exp[-z_i\phi(x)] \quad [\text{mol/m}^3] \qquad \text{(A5)}$$

with

$$\phi = q_e \cdot (\psi(x) - \psi(\infty))/kT \qquad \text{(A6)}$$

defined as the reduced potential. This equation applies to any ionic species i with charge $z_i q_e$, being subjected to the electrical field ($E = -d\psi/dx$), and describes the spatial equilibrium distribution of that ion. Considering only monovalent ions, combination of the two equations, eqs. A5 and A6 (with $\rho = \Sigma_i z_i F c_i$) yields the 'Poisson-Boltzmann' equation [60,61]:

$$d^2\phi/dx^2 = \kappa^2 \cdot \sinh(\phi(x)) \qquad \text{(A7)}$$

where

$$\kappa^2 = \frac{2q_e F c(\infty)}{kT\epsilon_w \epsilon_0} \qquad \text{(A8)}$$

$1/\kappa$ is the Debye-Hückel length [55] which amounts to 1 nm for an ionic strength of 100 mM and 10 nm for an ionic strength of 1 mM. It was assumed that at $x = \infty$ the solution becomes electroneutral, i.e. $c(\infty) = c^-(\infty) = c^+(\infty)$. The concentrations of H^+ and OH^- were assumed to be negligible relative to that of the salt.

With the appropriate additional assumptions (see below), the solution of this equation gives the equilibrium electrical potential profile and concomitant spatial ion distributions. The Poisson-Boltzmann equation can be solved analytically for

planar and cylindrical geometries. For spherical symmetries numerical methods are required [60].

To solve the one-dimensional Poisson-Boltzmann equation for our system with planar geometry (and also for stacked planar membranes as well as the spherical case, see appendices D and E), we apply the following assumptions [29]:

(1) The influence of the changes in pressure in the region of the charge accumulation is negligible.

(2) We consider an aqueous phase with only monovalent ions (KCl solution).

(3) The system is antisymmetrical around $x = 0$, where $x = 0$ refers to the middle of the membrane. This implies that $\psi(0) \overset{\text{def}}{=} 0$.

(4) At $x = \infty$: (a) $d\psi/dx = 0$, i.e., far from the membrane, the solution becomes electroneutral: $\rho \to 0$; $E \to 0$. (b) $\psi(\infty) = 0.5 \cdot \Delta\psi$, where $\Delta\psi$ is the bulk-to-bulk membrane potential, which is set to a certain value.

(5) Inside the membrane ($0 < x < r_m$): $\rho = 0$: $d^2\psi/dx^2 = 0 \to d\psi/dx = -E_m$ = independent of x.

(6) At the membrane-water transition ($x = r_m$): (a) ψ is continuous. (b) $\epsilon \cdot E$ is continuous:

$$\lim_{x \uparrow r_m} \left(\epsilon_m \frac{d\psi}{dx} \right) = \lim_{x \downarrow r_m} \left(\epsilon_w \frac{d\psi}{dx} \right) \tag{A9}$$

[14]. (In addition, in every phase ϵ_r is a constant in that phase.)

Using boundary conditions 1–6 the following solution for the non-linear Poisson-Boltzmann equation can be derived:

$$0 < x < r_m: \ \psi(x) = -E_m \cdot x \tag{A10}$$

$$r_m < x < \infty: \ \psi(x) = \psi(\infty) + \frac{4kT}{q_e} \cdot \operatorname{arctanh}\left\{ \left(\tanh\left[\frac{q_e(\psi(r_m) - \psi(\infty))}{4kT} \right] \right) \cdot \exp(-\kappa(x - r_m)) \right\} \tag{A11}$$

with $\psi(r_m)$ and E_m still unknown.

Applying boundary conditions 6a and 6b, $\psi(r_m)$ can be evaluated by use of the iteration method from the following formula:

$$\psi(r_m) + \frac{2kTr_m\epsilon_w}{\epsilon_m q_e} \cdot \sinh\left[\frac{q_e \cdot (\psi(r_m) - \psi(\infty))}{2kT} \right] = 0 \tag{A12}$$

Also, according to Gauss' Law E_m and σ can be related:

$$E_m = -\psi(r_m)/r_m = -\sigma/(\epsilon_m\epsilon_0) \tag{A13}$$

Finally, with eq. A5 the distribution of ions is evaluated.

For the linear Poisson-Boltzmann equation (which requires that $q_e(\psi(r_m) - \psi(\infty)) \ll kT$; i.e., $e^{\phi} \approx 1 + \phi$), the solution is much simpler:

$$0 < x < r_m: \ \psi(x) = \frac{\psi(\infty)}{(r_m + \epsilon_m/\epsilon_w\kappa)} \cdot x \tag{A14}$$

$$r_m < x < \infty: \ \psi(x) = \psi(\infty) \cdot \left[1 - \frac{\exp(-\kappa(x - r_m))}{(1 + r_m\epsilon_w\kappa/\epsilon_m)} \right] \tag{A15}$$

Appendix B: Buffered media

If, in addition to the non (pH) buffering monovalent salt, the aqueous media contain a buffer, the charged form of the buffer will contribute to charge density ρ. In general, this situation will not lead to the same Poisson-Boltzmann equation (eq. A7), but to equations that are more difficult to solve. However, there is a situation where a simple equation is obtained and we expect that this case shares most characteristics with the general case of complicated buffer mixtures. In this simplified situation, there is a mixture of buffer A and buffer B at equal total concentrations. The protonation equilibria and acid dissociation constants are defined by:

$$\begin{aligned} &A + H^+ \rightleftarrows A\text{-}H^+ && K_a = H^+ \cdot A/A\text{-}H^+ \\ &B + OH^- \rightleftarrows B\text{-}OH^- && K_b = OH^- \cdot B/B\text{-}OH^- \end{aligned} \tag{B1}$$

Consequently, the concentration of positive charges becomes:

$$\rho^+(x) = F \cdot (H^+(x) + A\text{-}H^+(x) + K^+(x)) = F \cdot [H^+(\infty) + A \cdot H^+(\infty)/K_a + K^+(\infty)] \cdot \exp(-\phi(x)) \quad [C/m^3] \tag{B2}$$

where $H^+(x)$ denotes the concentration of protons at location x, and similarly:

$$\rho^-(x) = F \cdot [OH^-(\infty) + B \cdot OH^-(\infty)/K_b + Cl^-(\infty)] \cdot \exp(\phi(x)) \quad [C/m^3] \tag{B3}$$

For simplicity, we assume pH 7 in the bulk phase (i.e., $OH^-(\infty) = H^+(\infty)$), and also assume $A/K_a = B/K_b$. Now the Poisson-Boltzmann equation becomes:

$$d^2\phi/dx^2 = \kappa_b^2 \cdot \sinh(\phi(x)) \tag{B3}$$

with again ϕ as reduced potential (eq. A6) and:

$$\kappa_b^2 = \frac{2q_e F[H^+(\infty) + A \cdot H^+(\infty)/K_a + K^+(\infty)]}{kT\epsilon_0} \tag{B4}$$

The solution of the Poisson-Boltzmann proceeds as described in appendix A.

In our calculations we used ϵ_w as the relative dielectric constant of the aqueous phase. It may be noted that the polarization of the buffer due to movement of protons from one buffer group to another [44] might also have been considered a part of an elevated ϵ_w. Since we are here focusing on the fraction of the charge accumulation that is due to protons, the present approach was more fruitful.

Appendix C: Protein layers

We consider two protein layers adjacent to the membrane, one on each side of it (see fig. 6). We assume the protein layer to be nearly impermeable for large ions such as K^+ and Cl^-, which leads to an equilibrium distribution over the protein and water phases according to $\Pi_K = [K_p^+/K_w^+]_{eq} \ll 1$, where Π_K is termed the partition coefficient. On the other hand, we assume the protein layer to be permeable for protons and OH^- (= H_2O minus H^+) due to the presence of hydration water and alkaline and acidic buffering groups in that layer. These buffering groups can become charged via the following reactions:

$$\begin{aligned} &\text{----A} + H^+ \rightleftarrows \text{----A-}H^+ \\ &\text{----B} + OH^- \rightleftarrows \text{----B-}OH^- \\ &K_a = [H^+ \cdot A/A\text{-}H^+]_{eq} \\ &K_b = [OH^- \cdot B/B\text{-}OH^-]_{eq} \end{aligned} \tag{C1}$$

Within the protein layer the treatment is analogous to that of the buffered media (cf. appendix B), except for terms involving partition coefficients for the ions between the protein layers and aqueous bulk phases. The concentration of positive charges in the protein becomes:

$$\rho^+(x) = F \cdot (H^+(x) + A\text{-}H^+(x) + K^+(x)) = F \cdot [H^+(\infty) + A \cdot H^+(\infty)/K_a + \Pi_K \cdot K^+(\infty)] \cdot \exp(-\phi(x)) \quad [C/m^3] \tag{C2}$$

where $H^+(x)$ denotes the concentration of protons at location x; and similarly:

$$\rho^-(x) = F \cdot [OH^-(\infty) + B \cdot OH^-(\infty)/K_b + \Pi_{Cl} \cdot Cl^-(\infty)] \cdot \exp(\phi(x)) \quad [C/m^3] \tag{C3}$$

For simplicity, we assume pH 7 in the bulk phase (i.e., $OH^-(\infty) = H^+(\infty)$), and also assume $A/K_a = B/K_b$ and $\Pi_K = \Pi_{Cl}$.

Now the Poisson-Boltzmann equation in the protein layer becomes:

$$d^2\phi/dx^2 = \kappa_p^2 \cdot \sinh(\phi(x)) \tag{C4}$$

with again ϕ as reduced potential (eq. A6) and:

$$\kappa_p^2 = \frac{2q_e F[H^+(\infty) + A \cdot H^+(\infty)/K_a + \Pi_K \cdot K^+(\infty)]}{kT\epsilon_p\epsilon_0} \quad [m^{-1}] \tag{C5}$$

Assuming, as before, no free charges in the membrane, $(d\psi/dx) = 0$ at $x = \infty$, and also allowing

linearization of the Poisson-Boltzmann equation, the following equations can be derived

$$0 < x < r_m: \quad \psi(x) = \alpha_1 \cdot x$$

$$r_m < x < r_p: \quad \psi(x) = \psi(\infty) + \frac{kT}{q_e}\alpha_2 \cdot \exp(\kappa_p x) + \frac{kT}{q_e}\alpha_3 \cdot \exp(-\kappa_p x) \qquad \text{(C7)}$$

$$r_p < x < \infty: \quad \psi(x) = \psi(\infty) + \frac{kT}{q_e}\alpha_4 \cdot \exp(-\kappa x) \qquad \text{(C8)}$$

α_1–α_4 were evaluated by applying the boundary conditions of continuity of both ψ and $\epsilon \cdot E$ at the membrane-protein ($x = r_m$) and protein-water ($x = r_p$) interphases.

In eq. C5 ϵ_p corresponds to the relative dielectric constant of the aqueous phase exclusive of the dielectric polarizability due to protons moving between buffer groups (the Kirkwood-Shumaker [44] contribution, cf. ref. 38). The latter is taken into account explicitly in keeping track of the spatial distribution of buffer-bound protons.

Appendix D: Stacked membranes

Many free-energy transducing membranes are not organized as a single flat membrane. In mitochondria and chloroplasts a large number of energy-coupling membranes are stacked. To determine the consequences that might occur for the spatial profile of the electric potential, we solved the Poisson-Boltzmann equation for the case depicted in fig. 4: an infinite array of membranes (hatched areas) of thickness d_m, which are separated by layers of aqueous medium of thickness $2l$. The polarity of the membranes (in terms of the direction in which their electron-transfer chains pump protons) alternates as indicated by the arrows. Again, for the aqueous layers the Poisson-Boltzmann equation is valid, whereas Poisson's equation applies throughout space. The only difference with the case of the single planar membrane concerns the boundary conditions. The condition that for x to $\pm\infty$, E must go to zero is replaced by the condition that E must equal zero halfway between every pair of neighbouring membranes, i.e., at $x = 0$, $\pm(2l + d_m)$, $\pm(4l + 2d_m)$, etc. Note that this does not imply that $\rho = 0$ at those locations. Once the potential profile between $x = 0$ and $x = l + (1/2)d_m$ has been calculated, the rest can be deduced from the symmetry properties of the system. The potential profile inside the membrane ($l < x < l + d_m$) is given by:

$$\psi(x) = \psi(l) + \sigma \cdot (x - l)/(\epsilon_m \epsilon_0) = \psi(l) + (x - l) \cdot \Delta\psi_m / d_m \qquad \text{(D1)}$$

Here σ is the amount of charge per unit surface area translocated across the membrane.

The potential in the aqueous phase between $x = 0$ and $x = l$ can be obtained by solving the Poisson-Boltzmann equation. The reference point for ψ has again been selected at $x = 0$. Since in this case the references ρ^+ and ρ^- are not equal, this equation cannot be reduced to eq. A7. Here we shall restrict ourselves to cases where, within every single aqueous phase, the reduced potential, ϕ, is small, such that the above equation can be linearized to yield:

$$\frac{d^2\psi}{dx^2} = \lambda + \kappa^2\psi \qquad \text{(D2)}$$

with:

$$\lambda = F \cdot (c^-(0) - c^+(0))/(\epsilon_w \epsilon_0) \qquad \text{(D3)}$$

and:

$$\kappa^2 = q_e F \cdot (c^+(0) + c^-(0))/(\epsilon_w \epsilon_0 kT) \qquad \text{(D4)}$$

(Since $c^-(0) - c^+(0) \ll c^+(0)$, we assume κ to be known.)

With the boundary conditions $\psi(0) = 0$ and $E(0) = 0$, the solution is:

$$\psi(x) = (\lambda/\kappa^2) \cdot (\cosh(\kappa x) - 1) \qquad \text{(D5)}$$

From eqs. A3, D4 and D5, the electric field strength at the membrane surface can be calculated:

$$E(l) = -(\lambda/\kappa) \cdot \sinh(\kappa l) \qquad \text{(D6)}$$

From the continuity of $\epsilon \cdot E$ one finds the relationship between λ, $c^-(0) - c^+(0)$ and the total

amount of translocated charge, σ (using eqs. A3, D1 and D6):

$$-\frac{\epsilon_m \epsilon_0 \Delta\psi_m}{d_m} = -\epsilon_w \epsilon_0 \frac{\lambda}{\kappa}\sinh(\kappa l) \tag{D7}$$

i.e.

$$\sigma = \frac{F\cdot(c^-(0)-c^+(0))\sinh(\kappa l)}{\kappa} \tag{D8}$$

and also:

$$\lambda = \frac{\Delta\psi_m \cdot \epsilon_m \cdot \kappa}{d_m \cdot \epsilon_w \cdot \sinh(\kappa l)} \tag{D9}$$

Substitution into eq. D5 gives:

$$\frac{\psi(x)}{\Delta\psi_m} = \frac{\epsilon_m \cdot (\cosh(\kappa x)-1)}{\epsilon_w \cdot \kappa \cdot d_m \cdot \sinh(\kappa l)} \tag{D10}$$

Using eq. A4, we find for the net charge density:

$$\rho = \frac{\Delta\psi_m \epsilon_0 \epsilon_m \kappa \cosh(\kappa x)}{d_m \sinh(\kappa l)} \quad (\mathrm{C/m^3}) \tag{D11}$$

Appendix E: Spherical vesicles

The Poisson-Boltzmann equation for spherically symmetric membrane systems cannot be solved analytically [60]. Thus, we consider the linearized case only. Let $\rho(r)$ denote the net (positive) charge density at r ($r=0$ signifying the center of the sphere). The Poisson equation for the system is (in spherical coordinates):

$$\begin{aligned} &0 < r \leqslant d_1, \quad d_2 \leqslant r < \infty: \\ &\nabla^2\psi(r) = -\rho(r)/(\epsilon_w \epsilon_0) \\ &d_1 < r < d_2: \\ &\nabla^2\psi(r) = 0 \end{aligned} \tag{E1}$$

Where d_1 and d_2 are the radii of the two membrane surfaces and

$$\nabla^2 \equiv \frac{1}{r^2}\frac{\mathrm{d}}{\mathrm{d}r} r^2 \frac{\mathrm{d}}{\mathrm{d}r}$$

Let $\psi(0)$, $c^+(0)$ and $c^-(0)$ be, respectively, the potential, positive ion concentration, and negative ion concentration at $r=0$, and $\psi(\infty)$, $c^+(\infty)$ and $c^-(\infty)$ be those at $r=\infty$. Then, the solutions of eq. E1, together with the Boltzmann equation can be obtained as:

$$0 < r \leqslant d_1: \qquad \psi(r) = \frac{\alpha_1}{r}e^{-\kappa r} + \frac{\beta_1}{r}e^{\kappa r} - \frac{\lambda}{\kappa^2} \tag{E2}$$

$$d_1 < r < d_2: \qquad \psi(r) = -\frac{\alpha_2}{r} + \beta_2 \tag{E3}$$

$$d_2 \leqslant r < \infty: \qquad \psi(r) = \frac{\alpha_3}{r}e^{-\kappa' r} + \frac{\lambda'}{(\kappa')^2} \tag{E4}$$

where κ and κ' are given by eqs. D4 and A8, respectively, and λ and λ' by:

$$\lambda = \frac{F\cdot(c^-(0)-c^+(0))}{(\epsilon_w \epsilon_0)} - \frac{q_e F \psi(0)(c^+(0)+c^-(0))}{(\epsilon_w \epsilon_0 kT)} \tag{E5}$$

$$\lambda' = \frac{F\cdot(c^+(\infty)-c^-(\infty))}{(\epsilon_w \epsilon_0)} + \frac{q_e F\cdot(c^+(\infty+c^-(\infty))\psi(\infty)}{(\epsilon_w \epsilon_0 kT)} \tag{E6}$$

The values of α_1, β_1, etc., are to be determined by the boundary conditions that include: (1) the continuity of potential and $\epsilon \cdot E$ at the two surfaces of the membrane; (2) the conservation of charges; (3) the given potential difference between points at the center of the sphere and at infinity; and (4) the average concentrations of ionic species inside and outside the sphere. After eqs. E2–E4 have been obtained, the charge density profile can be evaluated and used to calculate the net charge moved across the membrane (to produce the given potential difference).

Acknowledgements

We are indebted to Drs. Astumian, Azzone, Conover, van Dam, Hendler, Hill, Hellingwerf, Kell, Konings, Lemasters, Mitchell, Shrager, Walz and Williams for stimulating discussions and correspondence. Further, we thank Drs. Conover and Azzone for sending the manuscripts of two forth-

coming papers. This work was partly supported by the Netherlands Organization for the advancement of pure research (ZWO).

References

1 P. Mitchell, Nature 208 (1961) 147.
2 P. Mitchell, Chemiosmotic coupling in oxidative and photosynthetic phosphorylation (Glynn Research Ltd., Bodmin, Cornwall, 1966).
3 P. Mitchell, Chemiosmotic coupling and energy transduction (Glynn Research Ltd., Bodmin, Cornwall, 1968).
4 H.V. Westerhoff and K. van Dam, Thermodynamics and control of biological free-energy transduction (Elsevier, Amsterdam, 1987).
5 H.V. Westerhoff, B.A. Melandri, G. Venturoli, G.F. Azzone and D.B. Kell, Biochim. Biophys. Acta 768 (1984) 257.
6 S.J. Ferguson, Biochim. Biophys. Acta 811 (1985) 47.
7 H. Rottenberg, Modern Cell Biol. 4 (1985) 47.
8 E.C. Slater, J.A. Berden and M.A. Herweijer, Biochim. Biophys. Acta 811 (1985) 217.
9 P.D. Boyer, B. Chance, L. Ernster, P. Mitchell, E. Racker and E.C. Slater, Annu. Rev. Biochem. 46 (1977) 955.
10 L.A. Blumenfeld, Physics of bioenergetic processes (Springer-Verlag, Berlin, 1983).
11 W.N. Konings and G.T. Robillard, Proc. Natl. Acad. Sci. U.S.A. 79 (1982) 5480.
12 R.J.P. Williams, FEBS Lett. 53 (1975) 123.
13 P. Mitchell, FEBS Lett. 78 (1977) 1.
14 L.D. Landau, E.M. Lifshitz and L.P. Pitaevski, Electrodynamics of continuous media (Pergamon Press, Oxford, 1984).
15 P. Scholes and P. Mitchell, J. Bioenerg. 1 (1970) 309.
16 J.M. Gould and W.A. Cramer, J. Biol. Chem. 252 (1977) 5875.
17 D.B. Kell and G.D. Hitchens, Faraday Disc. Soc. 74 (1982) 377.
18 G.D. Hitchens and D.B. Kell, Biochim. Biophys. Acta 766 (1984) 222.
19 T.E. Conover and G.F. Azzone, in: Mitochondria and microsomes, eds. C.P. Lee, G. Schatz and G. Dallner (Addison-Wesley, Reading, MA, 1981) p. 481.
20 O.H. Setty, R.W. Hendler and R.I. Shrager, Biophys. J. 43 (1983) 371.
21 H.V. Westerhoff and Y. Chen, Proc. Natl. Acad. Sci. U.S.A. 82 (1985) 3222.
22 H.V. Westerhoff and F. Kamp, in: Organization of cell metabolism, eds. G.R. Welch and J.S. Clegg (Plenum, New York, 1987) p. 339.
23 M. Eisenbach and R. Caplan, Curr. Top. Membranes Transp. 12 (1979) 165.
24 W. Junge and A. Polle, Biochim. Biophys Acta 848 (1986) 265.
25 H.V. Westerhoff, Ph.D. Thesis, University of Amsterdam, The Netherlands (1983).
26 B. Ehrenberg, A. Lewis, T.K. Porta, J.F. Nagle and W. Stoeckenius, Proc. Natl. Acad. Sci. U.S.A. 77 (1980) 6571.
27 R. Heinrich, M. Gaestel and R. Glaser, J. Theor. Biol. 96 (1982) 211.
28 H. Ohshima and S. Ohki, Biophys. J. 47 (1985) 673.
29 P. Läuger, W. Lesslauer, E. Marti and J. Richter, Biochim. Biophys. Acta 135 (1967) 20.
30 H.G. Ferreira and M.W. Marshall, The biophysical basis of excitability (Cambridge University Press, Cambridge, U.K., 1985).
31 C.T. Everitt and D.A. Haydon, J. Theor. Biol. 18 (1968) 371.
32 S.H. White, Biochim. Biophys. Acta 323 (1973) 343.
33 J.J. Lemasters, FEBS Lett. 88 (1978) 10.
34 C.R. Hackenbrock, Trends Biochem. Sci. 6 (1981) 151.
35 R.A. Capaldi, Biochim. Biophys. Acta 694 (1982) 291.
36 P.A. Srere, in: Organized multienzyme systems, ed. G.R. Welch (Academic Press, New York, 1985) p. 1.
37 D.B. Kell and H.V. Westerhoff, in: Organized multienzyme systems ed. G.R. Welch (Academic Press, New York, 1985) p. 64.
38 R. Pethig, Dielectric and electronic properties of biological materials (J. Wiley, New York, 1979).
39 A.L. Koch, J. Theor. Biol. 120 (1986) 73.
40 D. Walz, EBEC Rep. 4 (1986) 341.
41 C.R. Hackenbrock, Proc. Natl. Acad. Sci. U.S.A. 61 (1968) 598.
42 S.W. Thorne and J.T. Duniec, Q. Rev. Biophys. 16 (1983) 197.
43 R.J.P. Williams, Trends Biochem. Sci. 8 (1983) 48.
44 J.G. Kirkwood and J.B. Shumaker, Proc. Natl. Acad. Sci. U.S.A. 38 (1952) 855.
45 T.L. Hill, Free energy transduction in biology (Academic Press, New York, 1977).
46 P.C. Maloney, J. Membrane Biol. 67 (1982) 1.
47 J. Boork and H. Wennerström, Biochim. Biophys. Acta 767 (1984) 314.
48 D. Pietrobon and S.R. Caplan, Biochemistry 24 (1985) 5764.
49 L.A. Blumenfeld, Problems of biological physics (Springer-Verlag, Berlin, 1981).
50 J.F. Myatt and J.B. Jackson, Biochim. Biophys. Acta 848 (1986) 212.
51 K. van Dam, A.H.C.A. Wiechmann, K.J. Hellingwerf, J.C. Arents and H.V. Westerhoff, Fed. Eur. Biochem. Soc. Symp. 45 (1978) 121.
52 P. Mitchell and J. Moyle, Biochem. J. 104 (1967) 588.
53 A. Warshel, S.T. Russell and A.K. Churg, Proc. Natl. Acad. Sci. U.S.A. 81 (1984) 4785.
54 M.K. Gilson, A. Rashin, R. Fine and B. Honig, J. Mol. Biol. 183 (1985) 503.
55 H.V. Westerhoff, EBEC Rep. 4 (1986) 8.
56 F. Kamp, R.D. Astumian and H.V. Westerhoff, Proc. Natl. Acad. Sci. U.S.A. 85 (1988) in the press.
57 D.B. Kell, R.D. Astumian and H.V. Westerhoff, Ferroelectrics (1988) in the press.
58 T.L. Hill, An introduction to statistical thermodynamics (Addison-Wesley, Reading, MA, 1960).
59 D.C. Grahame, Chem Rev. 41 (1947) 441.
60 D.Y.C. Chan and B. Halle, Biophys. J. 46 (1984) 387.
61 P.M.V. Resibois, Electrolyte theory (Harper & Row, New York, 1968).